MHD STREAMER STRUCTURE, SLOW SOLAR WIND, AND THE STREAMER BRIGHTNESS BOUNDARY

S. T. Suess[1], S. Nerney[2]

[1]NASA Marshall Space Flight Center/SD50, Huntsville, AL 35812, USA, ph. +1 256 544 7611, fax +1 256 544 5862, email steve.suess@msfc.nasa.gov
[2]Ohio University, 1570 Granville Pike, Lancaster, OH 43130, USA

ABSTRACT

Flow tubes adjacent to closed magnetic field lines on the boundaries of streamers can have spreading factors which change rapidly with height. Numerical models in this thin layer are subject to uncertainties. Here we use an analytic model of magnetically closed and adjacent open regions to analyze the spreading factor close to the closed field lines. The model is based on the one-temperature, isothermal flow model of Pneuman (1968), extended to calculate spreading factors and plasma beta, and to better explain streamer evolution with increasing temperature.

Key words: Streamers, Theory, MHD, Solar Wind

1. INTRODUCTION

Coronal streamers are bright because their density is higher than in adjacent regions of the corona. The boundary of streamers, the "brightness boundary" is often sharp and is sometimes thought of as being the interface between open (to the interplanetary medium) and closed magnetic field lines. However, this probably is not the case since the brightness boundary is commonly observed to extend even to the outer limits of the LASCO/C3 field of view — 30 solar radii (R_S) whereas static closed field lines do not extend past ~5 R_S in any published model.

Recently, Suess et al. (1999a) found that Ulysses observes only slow wind just inside the brightness boundary. It is therefore more likely that the brightness boundary and the fast/slow wind boundary are identical. This is supported by several independent lines of evidence, including: (i) A sharp velocity boundary in UVCS Doppler dimming data that apparently coincides with the brightness boundary (Habbal et al., 1997; Woo and Habbal, 1999). (ii) The sharp boundary between fast and slow wind in the interplanetary medium (McComas et al, 1998). (iii) The coincidence between first ionization potential (FIP) abundance anomalies and the fast/slow wind boundary at Ulysses (Geiss et al., 1996). (iv) The coincidence between UVCS-observed abundance anomalies in the legs of streamers and FIP abundance anomalies (Raymond et al. 1998). Raymond et al. furthermore concluded that slow wind originates in very slow or transient (on intervals of ~a day) releases or solar wind in the bright legs of streamers, just inside the brightness boundary. This is required for the gravitational settling that they infer exists.

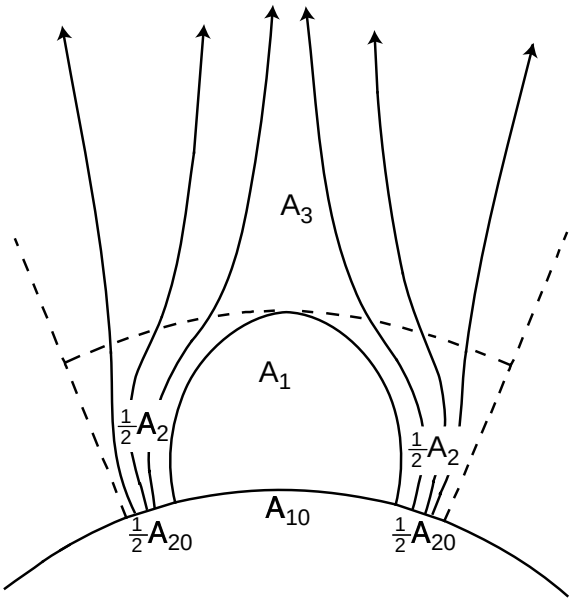

Fig. 1: Geometry assumed for the streamer model. A_1, A_2, and A_3 are described in the text.

Assuming the brightness and fast/slow wind boundaries are the same, it would be valuable to have a model of this region that can easily be used to analyze the different physical phenomena and questions that arise. In particular, we would like to be able to make a quantitative evaluation of the hypothesis by Noci et al. (1998) that slow wind arises because of the special properties of the geometric spreading factor along streamlines in complexes of otherwise closed streamer magnetic field regions. A 2d MHD model (V squez et al., 1999) has been used to find solutions like those proposed by Noci. Here we describe a simpler 1d model which promises to be able to do the same, but which we find cannot do so in its simplest form. Still, we are able to find new results on how streamer structure evolves under changing temperature and on the geometric spreading factor in the legs of streamers.

The model is based on the analysis of Pneuman (1968). Fig. 1 shows the geometry, assumed to be axisymmetric about the Sun and symmetric across the neutral line down the center of the streamer. A_{10} is the area of the base of the closed field lines in the streamer and A_{20} is the sum of the open, outflow areas on either side of the streamer. $A_1(r)$ and $A_2(r)$ are the areas of the regions 1 and 2 at constant height above the base at r_0. $A_3(r)$ is the area above the streamer. The dashed lines marking the outer boundaries of region 2 are assumed, in this example, to be radial so $A_3(r) \propto r^2$. We assume approximately radial flow and consider average values of the variables over the cross sections A_1 A_2, and A_3. This reduces the problem to 1d. We also assume that the gas is isothermal in regions 1 and 2 (a *two-temperature* model) and here we will consider only the simpler *one-temperature* model in which $T_1=T_2$. This closely follows Pneuman's analysis, although we extend his results and conclusions.

The assumption of hydrostatic equilibrium inside region 1 is based on the knowledge that β (the ratio of thermal

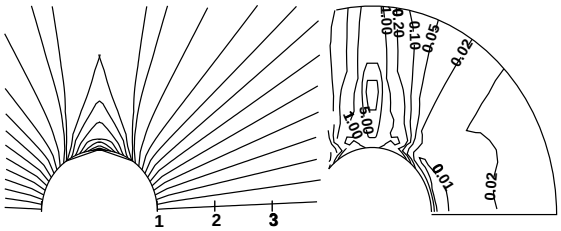

Fig. 2. Field lines (left) and β contours (right) from a recent MHD coronal model that shows $\beta>1$ throughout a streamer (Wang et al., 1998).

to magnetic pressure) is greater than unity in streamers above some low height of generally no more than 1.1-1.2 R_S (Suess et al., 1999b), which defines r_0 in the model. The closed field lines in the streamer are thus confined by the pressure from the magnetic field and plasma on adjacent open field lines pressing on the boundaries of the streamer (Suess and Smith, 1996). Empirical results from SOHO/UVCS and YOKHOH/SXT (Li et al., 1998; V squez et al., 1999) have empirically verified that $\beta>1$, but MHD models have long predicted this as a general property (Suess et al., 1999b). Because this is such an important and fundamental point for the viability of this analytic model, we show in Fig. 2 a typical numerical result for β. This model qualitatively reproduces the empirical bimodal (sharply divided fast and slow) solar wind (Phillips et al., 1995) and exhibits the property that the streamer is mainly confined by coronal hole field pressing on the streamer boundaries. $\beta>1$ throughout the streamer in this example.

2. ANALYSIS

The equations describing conditions in Fig. 1 are: (1) Hydrostatic pressure balance in region 1, with mean ion molecular weight μ and base radius (height) r_o.. We use μ=0.69 (20% alpha particles!) to compare with Pneuman (1968), who used the same value. (2) Radial momentum equation for isothermal Parker wind flow with an arbitrary geometric spreading factor in region 2. (3) Conservation of mass flux in region 2. (4) Conservation of magnetic flux in region 2 (B_{2o} and A_{2o} are the reference height magnetic field strength and cross-sectional area at r_o). (5) Conservation of total area $A_1(r)+A_2(r)$. (6) Pressure balance on the interface between regions 1 and 2.

$$N_1 = N_{10} \exp\left\{-\frac{\mu G M_8 m_p}{r_o k T_1}\left(1-\frac{r_o}{r}\right)\right\} \quad (1)$$

$$m_p N_2\left(V_2\frac{dV_2}{dr}+\frac{GM_8}{r^2}\right) = -\frac{kT_2}{\mu}\frac{dN_2}{dr} \quad (2)$$

$$N_2 V_2 A_2 = N_{2o} V_{2o} A_{2o} \quad (3)$$

$$B_2 A_2 = B_{2o} A_{2o} \quad (4)$$

$$A_1 + A_2 = \frac{r^2}{r_o^2}\left(A_{1o}+A_{2o}\right) \quad (5)$$

$$2kN_1T_1 = 2kN_2T_2 + \frac{1}{8\pi}B_2^2 \quad (6)$$

$p_2=2N_2kT_s$ and the dimensionless parameters are

$\psi=(\mu G M\ m_p)/(r_o k T_1)$	
$\tau=T_1/T_2$	Temperature Ratio
$R=A_{2o}/A_{1o}$	Area Ratio
$\beta=2N_{2o}kT_2/(B_{2o}^2/(8\pi))$	Plasma β
$N=N_{1o}/N_{2o}$	Density Ratio

(2) can be integrated and the equations solved analytically, with the requirement that the solution for V_2 pass through the critical point smoothly from subsonic flow close to the Sun to supersonic flow far from the Sun. In practice, the solution is generally more

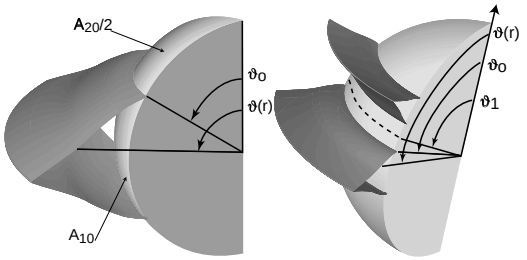

Fig. 3. Left: Areas A_{10} and A_{20} for open region A_{20} extending to the poles. Right: Areas A_{10} and A_{20} for the boundary outside A_{20} being limited by a mid-latitude streamer belt. The polar angle of the dashed radial line in Fig. 1 is defined as ϑ_1.

easily found by numerical integration of (2) in regions 2 and 3. A more detailed discussion of the solution will be given elsewhere, in a report on the *two-temperature* model ($\tau\neq1$). The reader is referred to Pneuman (1968) for details on how the *one-temperature* solution ($\tau=1$) is found. Here we report on the following properties from the *one-temperature* model: the height of the top of

closed region A_1; the *shape* of A_1; limits on temperature for A_1; the flow speed and spreading factors in A_2; and the plasma β in A_2.

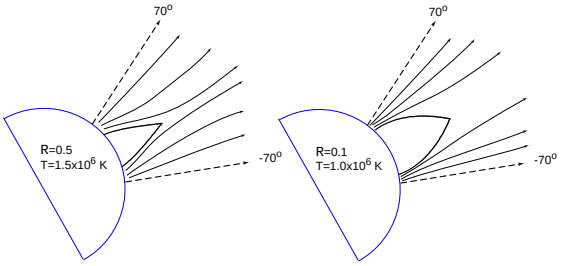

Fig. 4. The large size of R and higher temperature leads to a cusped helmet on the left, while a lower temperature and smaller R produces the domed helmet on the right.

Before continuing to results, the meaning of R, the Area Ratio, requires some explanation. The simplest concept is that there is a single streamer belt around the equator of the Sun and regions A_{20} extend to the north and south poles. This is shown in Fig. 3 (Left). However, the boundaries to A_{20} can be anywhere. Fig. 3 (Right) illustrates this, using a mid-latitude streamer belt to limit the region shown in Fig. 1. In general, we will take ϑ_1=70° in what follows. It is completely arbitrary, but

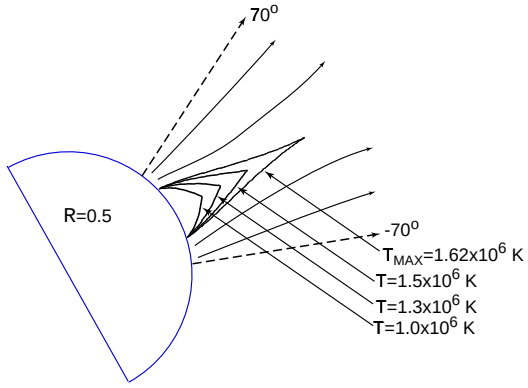

Fig. 5. Changes in helmet shape with increasing temperature, for fixed R. B_{20}=2.0 G, N_{20}=10^8 cm^{-3}. The helmet changes from domed, for T<1.3x10^6 K, to cusped for 1.3x10^6<T<1.62x10^6 K. Above 1.62x10^6 K there is no solution.

70° results in streamers of about the same base area as commonly observed. Then, the Area Ratio, R, gives ϑ_0 and we compute ϑ(r), the boundary of A_1(r), by solving (1)-(6). ϑ(r) is found as follows:

$$y_2(r) \equiv A_2(r)/A_{20}, \qquad y_1(r) \equiv A_1(r)/A_{10}$$
$$\vartheta(r) = \cos^{-1}\left[\cos\vartheta_1 / \left(1 + \mathsf{R} y_2(r)/y_1(r)\right)\right] \quad (7)$$

3. RESULTS

3.1. Helmet Geometry.

Given ϑ_1, we compute the boundary of $A_1(r)$ in terms of ϑ(r). Reviewing, first, some of Pneuman's results, he observed that the shape of the "helmet" derived from ϑ(r) takes on two forms — "domed" and "cusped" Fig. 4 shows this for B_{20}=2.0 G, N_{20}=10^8 cm^{-3}, r_0=6.96x10^{10} cm. The appearance depends on the choice of ϑ_1 but the general tendency is for the helmet to be short and

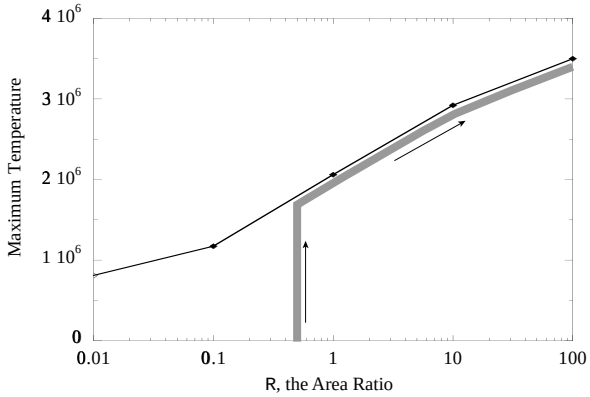

Fig. 6. The maximum temperature, for given Area Ratio R, above which no closed helmet solution exists. The gray evolutionary path is described in the text.

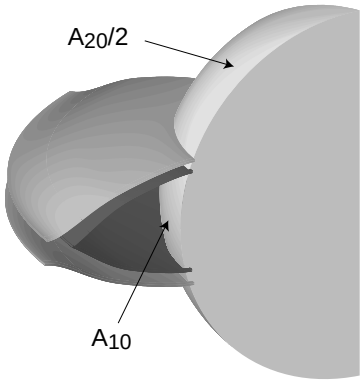

Fig. 7. As the temperature moves above T_{MAX}, closed helmets still can exist, but the basal area, A_{10}, must decrease. The result is a *narrower* helmet, large R, and higher permissable T_{MAX}.

domed either for low T_1 or large R. The reason low T_1 has this effect is intuitively obvious — the pressure in region 1 is therefore low. The reason large R has the same effect is that the surrounding region 2 area is relatively large and the helmet has to support the magnetic pressure exerted by this relatively large area. This is only possible for a relatively short, domed streamer.

An interesting result that follows from this is that, given a constant value of R, the helmet shape can be derived as a function of *T*. This is shown in Fig. 5, where a T_{MAX} of 1.62×10^6 K is indicated. Above this temperature there is no solution for constant R.

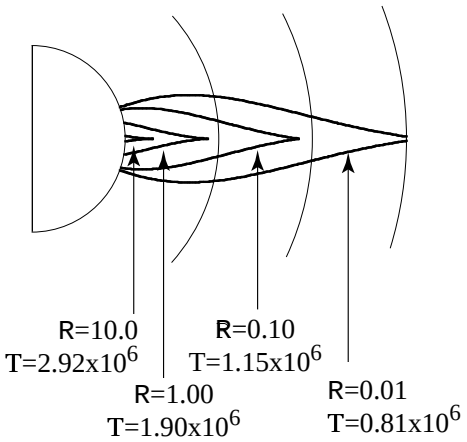

Fig. 8. How the Area Ratio, R, must increase when the temperature is increased past the T_{MAX} for the initial R.

Fig. 6 is a plot of the maximum temperature for which a solution exists *versus* the Area Ratio, R. This figure can be used to provide the interpretation of what happens if we assume that *T* increases past T_{MAX}. The gray line shows the evolutionary path for increasing temperature for arbitrary initial conditions. The direction of evolution, as the temperature increases, is shown by the arrows adjacent to the path. Referring in Fig. 5 and starting at a fixed R, the streamer height grows and changes from domed to cusped as the temperature increases. Then, when T_{MAX} is reached for the initial R, the outer part of the helmet is forced open. This is shown schematically in Fig. 7. The interpretation is that the temperature has become too high to support a helmet of the indicated height and therefore the basal area of the helmet has to decrease or, equivalently, R *increases*. For this reason, the gray evolutionary path in Fig. 6 moves to the right along the T_{MAX} curve after it meets that curve. Fig. 8 shows the effect on the helmet geometry when *T* increases, causing R to decrease. Finally, referring again to Fig. 6, there is an absolute maximum temperature of about 3.5×10^6 K, beyond which helmets cannot exist for solar conditions (mass, radius) under the assumption that $\beta > 1$ in region 1.

3.2. Flow Speed, Plasma β, and Spreading Factors.

Before showing results for flow speed, β, and spreading factor, *f*, recall that (2) is the equation for an isothermal Parker wind. Also, N_{10} is determined by the pressure balance from (6), together with B_{20}, N_{20}, and *T*. As B_{20} or N_{20} increases, the consequence is to increase N_{10}, but little else changes. Because of the isothermal Parker flow, density is decoupled from the flow speed. Therefore, changing N_{20} has no effect on flow speed. The solutions are dependent on only two parameters — R and *T*.

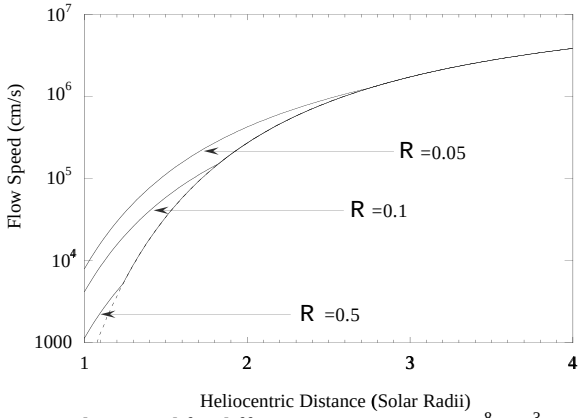

Fig. 9. Flow speed for different area ratios. $N_{10}=10^8$ cm^{-3}, $B_{20}=2$ G, $T=10^6$ K.

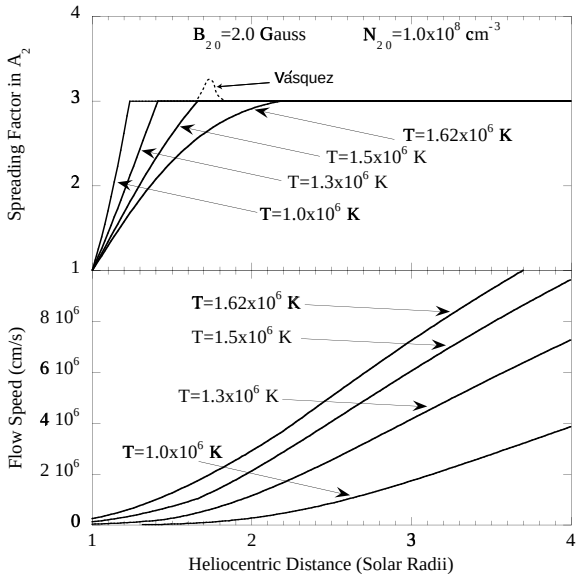

Fig. 10. Spreading factor and flow speed for the four cases illustrated in Fig. 5.

The dependence of V_2 on R is shown in Fig. 9, where the dashed line is the solution for spherically symmetric, isothermal flow ($R \to \infty$).

Fig. 9 illustrates that R has no effect on the ultimate flow speed in this kind of a model. However, *locally* the spreading can have a large effect. In this case, the flow around the helmet locally increases the speed. This effect is largest for the smallest R, corresponding to the smallest value for A_{20}. This kinematic effect is contrary to what seems to be required for gravitational settling, that is reduced flow speeds.

The total spreading, f_{TOT}, between r_0 and the top of the helmet is easily computed from R for this problem. If

we take the top of the helmet to be at a height r_h, f_{TOT} is found from:

$$A(r_h) = A_{10} + A_{20}$$
$$f_{TOT} = A(r_h) / A_{20} = 1 + 1/R \quad (8)$$

So f_{TOT}=21, 11, and 3 for the three examples in Fig. 9, for R=0.05, 0.1, and 0.5 respectively. As would be expected for isothermal flow, the density profiles are the same for all three of these solutions.

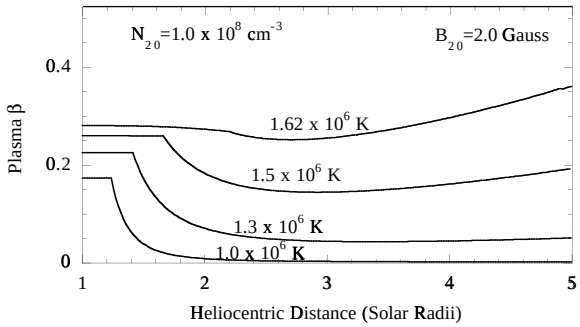

Fig. 11. Plasma β for the cases shown in Figs. 5 and 10.

Fig. 10 shows the effect of changing temperature on the flow speed solution. The heights of the helmet in this example, for the same temperatures, can be seen in Fig. 5. The total spreading, f_{TOT}, is constant by (8), but the rate of change of *f(r)* with height changes as the height of the helmet increases. For the very lowest helmets (low *T*), *f(r)* increases from 1 to 3 over only 0.2 R_S. This is less extreme than the increase in spreading seen at the base of plumes (Suess et al., 1998), a potentially related phenomenon. Comparing this with *f(r)* from V squez et al. (1999) shows that their transition to slow flow occurs because of a specific behavior in *f* near the top of the streamer — it locally increases above the asymptotic value and then decreases back down to the asymptotic value over a height of less than 1 R_S. This is schematically shown by the dashed line in Fig. 10 marked ÒV squezÓ The flow is apparently choked off in their model by the local increase and subsequent decrease in spreading.

The flow speed at 4 R_S in Fig. 10 ranges from 40 to slightly more than 100 km/s. In contrast, coronal hole speeds at this height are 300-600 km/s (Casalbuoni et al., 1999). Therefore, the flow in region 2 in the *one-temperature* model is not like coronal hole flow. Because the base density, N_{10}, is 10^8, the density in region 2 is not significantly different than in a coronal hole but the lack of coupling between flow and density in the isothermal model restricts the utility of making any deductions from the model density. However, one interesting point does appear. Namely the plasma β in region 2 is not large. β for the four cases shown in Figs. 5 and 10 is plotted in Fig. 11.

Whether β<1 or β>1 in region 2 raises interesting questions. If β>1, as seems to be the case if region 2 is *inside the brightness boundary*, then an additional low β region (region 4), outside region 2, might be added to this model to take coronal hole flow into account. Conversely, if β<1, as for coronal hole flow, then the the plasma has little influence on the solution.

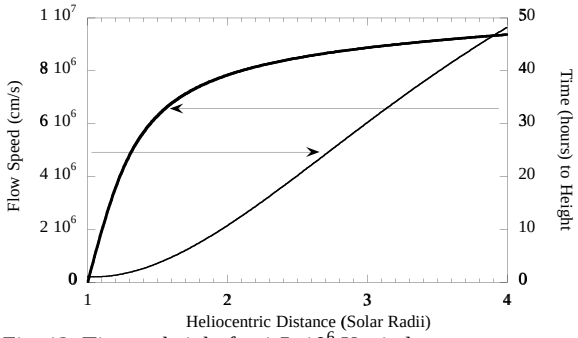

Fig. 12: Time to height for $1.5x10^6$ K wind.

The solution in region 2 is similar to what is believed to exist for slow solar wind. The flow speed is low (Fig. 10) and the density if relatively high. In this case, it is of interest to know the transit time of the flow through the corona. This is shown in Fig. 12 for the $1.5x10^6$ K wind, where it is seen that it takes ~2 days for plasma to pass from 1 to 4 R_S. This is an interesting number in view of the limitations described by Raymond et al. (1998) on flow in the boundaries of streamers if the observed amount of gravitational settling is to be achieved. They speculate that ÖThe observed enhancement of oxygen abundance in the streamer legs is due to Émixing which refreshes the material in the legs on a time scale of 1 day or less.ÓThe slow flow and long transit time illustrated in Fig. 12 appear to meet this requirement.

To extend the one-temperature model to allow investigation of multiple solution topologies like that found by V squez et al. (1999) will probably require some or all of the following: (i) Extension to two temperatures. (ii) Addition of a region 4, representing low β coronal hole flow outside the brightness boundary. (iii) Generalization away from a simple Parker flow model so that density and flow speed are coupled.

4. SUMMARY & CONCLUSIONS

We describe a simple model of streamer structure which incorporates the major morphologic properties of streamers. The present version of the model (Pneuman, 1968) uses assumptions which oversimplify the problem, but which still lead to new physical insight.

First, it predicts how a streamer evolves under continuously increasing temperature. There is an absolute maximum temperature of ~3.5×10^6 K beyond which isothermal streamers do not exist on the Sun, under the assumption that $\beta>1$ in region 1. Branching solutions between fast and slow wind, for increasing spreading factors, are not obtained in this simple model. In V squez et al.õs (1999) model, the spreading factor behavior, which is reproduced schematically here in Fig. 10, occurs where $\beta<1$ and where the kinetic energy is also less than the magnetic field energy density. Therefore, simply adding the region 4 described above will probably recover this behavior.

Finally, it appears that the radial dashed line in Fig. 1, bounding region 2, can now be interpreted as the brightness boundary, as opposed to being in the center of a coronal hole as supposed by Pneuman (1968).

ACKNOWLEDGEMENTS

We would like to thank Roger Kopp for directing our attention to Pneumanõs (1968) early work as a way of developing simple but useful analytic models of streamers. This research was supported by the UVCS/SOHO and SWOOPS/Ulysses experiments.

REFERENCES

Casalbuoni, S., L. Del Zanna, S. R. Habbal, and M. Velli, 1999: Coronal plumes and the expansion of pressure-balanced structures in the fast solar wind, *J. Geophys. Res., 104*, 9947-9961.

Geiss, J., and 10 others, 1996: The southern high-speed stream: Results from the SWICS instrument on Ulysses, *Nature, 268*, 1033-1036.

Habbal, S. R., R. Woo, S. Fineschi, R. OõNeal, J. Kohl, G. Noci, and C. Korendyke, 1997: Origins of the slow and the ubiquitous fast solar wind, *Astrophys. J. Lett., 489*, L103-L106.

Li, J., J. C. Raymond, L. W. Acton, et al.: 1998, Physical Structure of a Coronal Streamer in the Closed-Field Region as Observed from UVCS/SOHO and SXT/YOHKOH, *Astrophys. J., 506*, 431.

McComas, D. J., P. Riley, J. T. Gosling, A. Balogh, and R. Forsyth, 1998: Ulysses rapid crossing of the polar coronal hole boundary, *J. Geophys. Res., 103*, 1955.

Noci, G., and 24 others, 1998: The quiescent corona and slow solar wind, in *The Corona and the Solar Wind Near Minimum Activity*, ESA SP-404, 75-84, ESA Publications Division, Noordwijk, The Netherlands.

Phillips, J. L., S. J. Bame, W. C. Feldman, B. E. Goldstein, J. T. Gosling, C. M. Hammond, D. J. McComas, M. Neugebauer, E. D. Scime, & S. T. Suess, 1995: Ulysses solar wind plasma observations at high southerly latitudes, *Science, 268*, 1030.

Pneuman, G., 1968: Some general properties of helmeted coronal structures, *Sol. Phys., 3*, 578.

Raymond, J., R. Sulieman, A.van Ballegooijen, and J. Kohl, 1998: Absolute abundances in streamers from UVCS, in *Correlated Phenomena at the Sun, in the Heliosphere, and in Geospace*, Proc. 31st ESLAB Symp., ESA publ. SP-415, ESA Publications Div., Noodrwijk, The Netherlands.

Suess, S.T., and Smith, E.J. 1996, Latitudinal dependence of the radial IMF component: coronal imprint, *Geophsy.Res.Lett., 23*, 3267.

Suess, S. T., G. Poletto, A.-H. Wang, S. T. Wu, & I. Cuseri, 1998: The geometric spreading of coronal plumes and coronal holes, *Sol. Phys., 180*, 231.

Suess, S. T., G. Poletto, G. Corti, G. Simnett, G. Noci, R. Romoli, J. Kohl, and B. Goldstein, 1999a: Ulysses — UVCS coordinated observations,*Space Sci. Rev.*, in press.

Suess, S. T., G. A. Gary, and S. F. Nerney, 1999b: β in streamers, in *Solar Wind Nine* (S. R. Habbal, R. Esser, J. V. Hollweg, and P. A. Isenberg, eds.), 247-250, AIP Conf. Proc. 471, Woodbury, New York.

V squez, A. M., A. A. van Ballegooijen, and J. C. Raymond, 1999: Model of solar wind flow near an equatorial coronal streamer, in *Solar Wind Nine*, (S. R. Habbal, R. Esser, J. V. Hollweg, and P. A. Isenberg, eds.), 243-246, AIP Conf. Proc. 471, Woodbury, New York.

Wang, A.-H., S. T. Wu, S. T. Suess, and G. Poletto, 1998: Global model of the corona with heat and momentum addition, *J. Geophys. Res., 103*, 1913-1922.

Woo, R., and S. R. Habbal, 1999: A new view of the origin of the solar wind, in *Solar Wind Nine*, (S. R. Habbal, R. Esser, J. V. Hollweg, and P. A. Isenberg, eds.), 71-76, AIP Conf. Proc. 471, Woodbury, New York.